Subiculum–entorhinal cortex interactions during *in vitro* ictogenesis

Rochelle Herrington[a,b], **Maxime Lévesque**[a,b], and **Massimo Avoli**[a,b,c,*]

[a]Montreal Neurological Institute, McGill University, H3A 2B4 Montréal, QC, Canada

[b]Department of Neurology and Neurosurgery, McGill University, H3A 2B4 Montréal, QC, Canada

[c]Department of Physiology, McGill University, H3A 2B4 Montréal, QC, Canada

Abstract

Purpose—Our aim was to establish the contribution of neuronal networks located in the entorhinal cortex (EC) and subiculum to the generation of interictal and ictal onset patterns recorded *in vitro*.

Methods—We employed field potential recordings of epileptiform activity in rat brain slices induced with the application of the K^+ channel blocker 4-aminopyridine. Local connections between the EC and subiculum were severed to understand how EC–subicular circuits contribute to patterns of epileptiform synchronization.

Results—First, we found that ictal discharges occurred synchronously in these two structures, initiating from either the EC or subiculum, and were characterized by *low voltage fast* (LVF) or *sudden* onsets. Second, sudden onset ictal events initiated more frequently in the EC, whereas LVF onset ictal discharges appeared more likely to initiate in the subiculum ($P < 0.001$). In both structures, polyspike interictal discharges occurred in brain slices generating sudden onset ictal events while isolated slow interictal discharges were recorded in experiments characterized by LVF onset ictal activity. Third, severing the connections between subiculum and EC desynchronized both interictal and ictal discharges occurring in these two regions, leading to a significant decrease in ictal duration (regardless of the onset type) along with blockade of polyspike interictal activity in subiculum.

Conclusions—These findings highlight the contribution of EC–subicular interactions to epileptiform synchronization and, specifically, to ictogenesis in this *in vitro* model.

Keywords

4-Aminopyridine; Sudden onset; Low-voltage fast onset; Entorhinal cortex; Subiculum

*Corresponding author at: Montreal Neurological Institute, McGill University, 3801 University Street, H3A 2B4 Montréal, QC, Canada. Tel.: +1 514 998 6790/+39 333 483 1060; fax: +1 514 398 8106. avoli@mcgill.ca (M. Avoli).

Conflict of interest
The authors declare no conflict of interest.

1. Introduction

Focal seizures can be classified according to their region of onset as well as to their onset pattern. Studies performed in temporal lobe epilepsy patients have revealed the existence of two main types of seizure onset patterns that have been termed hypersynchronous and low voltage fast (LVF) [1,2]. These seizure onset patterns, which have also been observed in animal models of temporal lobe epilepsy *in vivo* [3,4], may reflect the contribution of distinct mechanisms of ictogenesis. Moreover, *in vitro* studies performed in rodent brain slices comprising the hippocampus and the entorhinal cortex (EC) during application of the K^+ channel blocker 4-aminopyridine (4AP) have revealed the presence of LVF or sudden ictal onset patterns in the EC [5]. Hypersynchronous onset discharges were detected in the EC as well, but this pattern was limited to only a few cases [5].

In this study, we analysed for the first time the contribution of the interactions between the EC and the subiculum to the synchronous epileptiform activity induced by 4AP *in vitro.* The EC is implicated as one of the possible seizure onset regions in temporal lobe epilepsy [4,6], and presents with epileptogenic changes in both humans and animal models mimicking this disorder [7,8]. In contrast to the EC, the subiculum of temporal lobe epileptic patients presenting with hippocampal sclerosis shows little to no neuronal damage [7–9]. In addition, *in vivo* studies have demonstrated its involvement in seizure onset in models of temporal lobe epilepsy [6]. Finally, tissue resected from the subiculum of patients with temporal lobe epilepsy generates spontaneous interictal-like (from hereafter termed interictal) discharges [10], but it is unable to generate spontaneously occurring ictal discharges [11]. Using the *in vitro* 4AP model of epileptiform synchronization, we employed in this study field potential recordings to investigate the involvement of the subiculum in the ictogenic processes that lead to the generation of LVF or sudden ictal onset patterns in the EC.

2. Materials and methods

2.1. Slice preparation and maintenance

All procedures were performed in accordance with and approved by the Canadian Council of Animal Care and the McGill Animal Care Committee. All efforts were made to minimize the suffering and number of animals used. Male Sprague-Dawley rats (175–250 g; Charles River Laboratories, Saint Constant, QC, Canada) were decapitated under isoflurane anaesthesia (Baxter Corporation, Mississauga, ON, Canada). The brain was quickly removed and placed in ice cold, oxygenated artificial cerebrospinal fluid (ACSF) with the following composition: 124 mM NaCl, 2 mM KCl, 2 mM $CaCl_2$, 2 mM $MgSO_4$, 1.25 mM KH_2PO_4, 26 mM $NaHCO_3$, and 10 mM D-glucose. The ACSF was continuously bubbled with an O_2/CO_2 (95/5%) gas mixture to maintain the pH at 7.4. The cerebellum was severed and the brain was mounted for slicing. Slices with a thickness of 450 μm were obtained with a vibratome (VT1000S; Leica, Concord, ON, Canada) and transferred to an interface chamber. Slices were maintained between warm (32 ± 1 °C) ACSF (pH 7.4, 305 mOSM/kg) and humidified gas (O_2/CO_2, 95%/5%). Following a recovery period of at least 1 h, epileptiform activity was induced by continuous bath application of 4AP (50 μM; Sigma–Aldrich, Oakville, ON, Canada) at a flow rate of 2 mL/min.

The EC and subiculum were continuously recorded during 4AP application for a period of up to 90 min. In cut experiments, a scalpel blade mounted on a micromanipulator was used to sever the connections between the EC and subiculum. NMDA receptor mediated signalling was blocked by applying 10 μM 3-(2-carboxypiperazin-4-yl) propyl-1-phosphonic acid (CPP; Tocris Bioscience, Ellisville, MO, USA). Recordings were analysed beginning 30 min following 4AP application, immediately following the recovery of spontaneous epileptiform activity after cut experiments, and 10 min following CPP application.

2.2. Field potential recordings

Field potential recordings were obtained with ACSF-filled glass pipettes (1B150F-4; World Precision Instruments, Sarasota, FL, USA; tip diameter <10 μm; resistance 5–10 MΩ) pulled by a Sutter P-97 electrode puller (Sutter, Novato, CA, USA). Signals were fed to an AI 401 amplifier and a CyberAmp 380 (Molecular Devices, Silicon Valley, CA, USA). Traces were digitized using a Digidata 1322A (Molecular Devices). Signals were sampled at 5 kHz and cut off at 1 kHz.

2.3. Statistics and analysis

Analysis of field potential recordings was performed offline with CLAMPFIT 8.2 (Molecular Devices) and reviewers were blind to the regions being analysed and treatment applied to the slice. Throughout this study, we arbitrarily termed as 'ictal' or 'interictal' the synchronous epileptiform events longer or shorter than 3 s, respectively (*cf.*, [12]). The normal distribution of data was tested with Skewness and Kurtosis tests. Data were analysed with either two-way ANOVA followed by Tukey's multiple comparisons test, or with Student's *t*-test. Fisher's Exact Test was used to determine whether non-random associations existed between two categorical variables. Throughout the text, n indicates the number of slices studied, unless otherwise specified. Results are expressed as mean ± standard error of the mean. Results were considered to be significantly different at $P < 0.05$.

Sudden onset discharges arose abruptly from a frequent polyspike interictal background (arrows in Fig. 1A) while LVF events initiated with a pattern of low-voltage fast activity occurring at approx. 10–20 Hz (arrows in Fig. 1B) (*cf.*, [5]). The onset of the interictal events was determined to be the first deflection from the baseline. To determine the delays occurring between the EC and subiculum during ictal or interictal events, while blind to the region, cursors were placed at the onset of the respective ictal events. The time delay was then calculated by built-in software provided by CLAMPFIT 8.2. Following analysis, delays were reassigned based on the regions of onset with negative values arbitrarily defined to initiate from the subiculum and positive values to initiate from the EC.

3. Results

3.1. 4AP induced ictal discharges

A total of 84 ictal events from 31 brain slices were recorded simultaneously from the EC and subiculum (Fig. 1A and B). Forty-six of these ictal events appeared to initiate in the subiculum, 38 in the EC, and one had simultaneous onset in both regions (Fig. 1C). When ictal events initiated from the EC, ictal duration averaged 73.8 ± 5.6 s in the EC and 66.3

± 4.3 s in the subiculum ($n = 46$ events) (Fig. 1D). When events initiated from the subiculum, ictal duration averaged 87.3 ± 5.4 s in the EC and 76.8 ± 5.3 s in the subiculum ($n = 38$ events) (Fig. 1D). There was no significant difference between these values.

To understand the relationship between regions and patterns of ictal onset, we categorized ictal discharges by their onset pattern. From the total number of ictal events recorded, 51 were characterized as sudden onset events ($n = 17$ slices); 33 of these ictal discharges were found to initiate from the EC while 18 appeared to initiate from the subiculum. A total of 33 LVF onset ictal discharges ($n = 13$ slices) were recorded; 9 were found to initiate from the EC and 24 from the subiculum (Fig. 1E). Both sudden and LVF onset events could be recorded from slices obtained from a single animal, but ictal onset patterns remained constant within a given slice.

Overall, suddenly arising ictal events were more likely to initiate in the EC area while LVF onset ictal events most frequently initiated from the subiculum (Fisher's Exact Test; $P > 0.001$). The average delay between the start of ictal activity in the EC and subiculum based on the type of ictal onset, irrespective of the region where the ictal event was first detected, was 162.1 ± 136.2 ms for sudden onset ictal events ($n = 51$ discharges) and -517.4 ± 340.5 ms for LVF onset events ($n = 33$ discharges). These values were found to be significantly different from each other thus reinforcing the evidence that the EC was more likely to initiate sudden onset ictal events whereas the subiculum was more frequently initiating LVF onset events ($P < 0.001$) (see also Fig. 2E).

3.2. Interictal patterns preceding ictal events

Two patterns of interictal activity were closely associated with the two ictal onset patterns (Fig. 2A and B) [5]. In both cases, interictal events occurred at the same frequency and with similar duration in the EC and subiculum within a given slice; therefore, data were pooled together. Suddenly arising ictal discharges were accompanied by frequent polyspike interictal discharges, which were characterized by an average duration of 0.7 ± 0.1 s and an average interval of 2.7 ± 0.6 s ($n = 17$ slices) (Fig. 2C). LVF onset ictal events were associated with isolated slow interictal discharges, which were characterized by longer durations (1.2 ± 0.2 s; $P = 0.017$) and intervals of occurrence (26.0 ± 4.8 s; $P = 4.8$ E–5) ($n = 13$ slices) compared to frequent polyspike interictal discharges (Fig. 2C).

The delays detected between the initiation of interictal events in the EC and subiculum were less pronounced compared to the initiation delays associated with the ictal onset. In the interictal event preceding the start of the ictal discharge, fast polyspike interictal discharge delays were distributed around 0, whereas isolated slow interictal delays were shifted towards more negative values (Fig. 2D); such negative values indicated that the onset of slow interictal discharges, like their associated ictal events, were more likely to initiate around the subiculum. To better understand the dynamics of jittering between the EC and subiculum, we assessed the delays for a period of 50 s in 10 s bins before the last interictal event preceding ictal onset (Fig. 2E). On average, isolated slow interictal discharge delays were found to be more negative compared to fast polyspike interictal discharge delays, further suggesting that isolated slow discharges were more likely to initiate in the subiculum. Compared to the ictal onset, interictal delays remained more closely around 0. We also

expanded the 10 s epoch leading up to the ictal event in cases of sudden onset discharges to see whether changes existed on a smaller scale (inset in Fig. 2E) but we could not find any predictive changes in interictal delay times that herald the onset of the ictal event. However, we saw that these delays jittered around 0 in a pattern that was characterized by a frequency of approximately 0.2 Hz. Overall, interictal delays did not appear to be predictive of ictal onset and ictal onset delays were longer than those associated with interictal delays.

3.3. Surgical cut between entorhinal cortex and subiculum

In a subset of eight slices, the connections between the EC and subiculum were severed following 30 min of control recordings (Fig. 3C). In slices characterized by suddenly arising ictal discharges ($n = 5$ slices), cutting the connections desynchronized the epileptiform synchronous events occurring in these two structures (Fig. 3A). In two of five slices, ictal events disappeared from the subiculum while they continued to occur in the EC but with a marked reduction in duration compared to control ($P = 0.034$) (Fig. 3A, +Cut, panel a). In the remaining experiments ($n = 3$) a series of continuous spikes at 1–1.5 Hz lasting for several tens of seconds could be recorded from the subiculum following isolation from the EC (Fig. 3A, +Cut, identified by a dotted line in panel b); it should be emphasized that this continuous spike pattern lacked any tonic–clonic component as identified in typical ictal discharges and, in contrast to what observed before the cut, they were characterized by positive-going electrographic elements. The duration and the interval of occurrence of sudden onset ictal discharges recorded in the EC under control conditions and following the cut are plotted in Fig. 3D and E.

LVF onset ictal discharges were also influenced by severing the connections between the EC and subiculum ($n = 3$ slices) (Fig. 3B). After the cut, ictal events with LVF onset characteristics continued to occur in the EC with shorter duration ($P < 0.05$) but at non-significantly different rates of occurrence compared to control (Fig. 3B, +Cut, panel a). In contrast, ictal discharges were abolished in the subiculum where they were replaced by a pattern of continuous positive-going spikes at 1–1.5 Hz similar to what is seen in brain slices generating sudden onset ictal activity following cut (Fig. 3B, +Cut, identified with a dotted line in panel b). The duration and the interval of occurrence of LVF onset ictal discharges recorded in the EC under control conditions and following the cut are plotted in Fig. 3D and E.

As illustrated in Fig. 4, following the cut, interictal events recorded in the EC and subiculum were also desynchronized (Fig. 4A and B). In slices generating sudden onset ictal discharges, the duration of interictal events in the subiculum increased after cut ($n = 5$ slices; $P < 0.001$) but did not significantly change in the EC (Fig. 4C). The interval between interictal events increased after the cut in both the EC and subiculum ($n = 5$ slices; $P < 0.001$), but the increase was greatest in the subiculum ($P < 0.001$) (Fig. 4D). Furthermore, while frequent polyspike interictal discharges persisted in the EC following the cut, they disappeared in the subiculum and were replaced by slow interictal discharges similar to those recorded from brain slices generating LVF onset patterns (Fig. 4A, double arrow). In slices characterized by LVF onset ictal discharges, the duration of interictal discharges in the EC increased after the cut ($n = 3$ slices; $P < 0.001$) while in the subiculum there was not

significant change (Fig. 4C). Moreover, as illustrated in Fig. 4D, the interval of occurrence of the interictal events recorded from the EC and subiculum decreased following the cut ($n = 3$ slices; $P < 0.001$) (Fig. 4D). Overall, these findings indicate that the EC is able to sustain both polyspike and long-lasting interictal discharges, whereas the subiculum can only sustain long lasting interictal discharges when the two regions are disconnected.

3.4. Application of an NMDA receptor antagonist

Finally, to establish the role of NMDA receptor mediated signalling in epileptiform activity recorded from the EC and subiculum following the severance of connections between the two regions, we applied 10 μM CPP to brain slices that were generating either sudden or LVF onset ictal discharges before the cut. Ictal events remaining in the EC as well as the trains of positive-going spikes at 1–1.5 Hz persisting in the subiculum after the cut were abolished by CPP (not illustrated). Therefore, we focused on the analysis of the changes induced by this NMDA receptor antagonist on interictal activity generated by the isolated EC and subiculum.

In brain slices that were characterized by sudden onset ictal discharges, CPP did not change the duration of the polyspike interictal discharges in the EC (Fig. 5C) while their interval of occurrence increased significantly and became irregular ($n = 5$; $P < 0.05$) thus disrupting the rhythmicity of this type of interictal pattern (Fig. 5D); in addition, in these experiments field oscillations at approx. 2 Hz, which followed each interictal discharge, emerged during NMDA receptor antagonism (arrows and insert in Fig. 5A, +CPP). In the subiculum, the interval of occurrence and the duration ($n = 3$; $P < 0.05$) of the long lasting interictal events increased significantly in the presence of CPP (Fig. 5C and D). In those brain slices in which LVF onset seizures occurred before the cut, CPP did not change the duration of the interictal events recorded in EC but significantly increased their interval of occurrence ($n = 3$; $P < 0.05$) (Fig. 5C and D); in addition, we found in these experiments that CPP decreased the duration of the long-lasting interictal events recorded in the subiculum ($n = 3$; $P < 0.001$) without significantly affecting their interval of occurrence (Fig. 5C and D).

4. Discussion

The main findings of this study can be summarized as follows. First, in intact brain slices suddenly arising ictal events predominantly initiate in the EC whereas LVF onset ictal events often appear to initiate from the subiculum. Second, in spite of such apparent subicular initiation of LVF ictal activity, severing the connections between EC and subiculum abolishes ictogenesis in the latter structure. Third, we confirmed the application of the NMDA receptor antagonist CPP could block the occurrence of both sudden and LVF onset ictal events in the EC as well as the fast trains of spikes generated by the isolated subiculum after cut. Fourth, CPP disrupted the rhythmicity of fast polyspike interictal discharges in the EC following cut.

4.1. Contribution of entorhinal cortex–subiculum interactions to ictogenesis

Within the limbic system, the subiculum holds a strategic position as an interface between the hippocampus proper and parahippocampal structures. It serves as the major output

structure of the hippocampus, receiving extensive projections from the CA1 hippocampal region [13,14] and projecting towards both extralimbic and limbic areas including the thalamus [15,16], perirhinal cortex [14], amygdala [16] and EC [17]. While the subiculum acts as the output structure of the hippocampus, the EC provides afferents to the hippocampus *via* the perforant path [18,19]. The perforant pathway plays an important role in epileptic disorders but there also exists an additional entorhinal input to the subiculum [20,21]. This short EC–subicular, subicular–EC circuit through temporoammonic pathway, is functionally active thus suggesting that hippocampal inputs and outputs can be modulated locally between these two regions [20,22].

In the current study, we found evidence suggesting that this local EC–subicular circuit plays an important role in the synchronization and maintenance of ictal activity while in a previous study from our laboratory, the subiculum was found to function as the gating structure acting between the hippocampus proper and the EC [23]. According to this early experiments, as long as GABA$_A$ receptor-mediated signalling was maintained, the subiculum effectively "blocked" the further propagation of CA3-driven interictal discharges to the EC, and it generated interictal events that occurred synchronously with those recorded in the CA1–CA3 subfields [23]. These different results may depend on slightly different slicing procedures such as the angle of approx. 10° used to orient the brain tissue before obtaining horizontal slices (*cf.*, [23,24]). This view is supported by the fact that in these early studies the majority of the epileptiform patterns recorded from the EC during 4AP application consisted of isolated, long lasting interictal discharges along with LVF onset ictal events while the sudden onset pattern described here (as well as in [5]) was rarely seen. Another factor contributing to the ability of subicular networks to generate and actually initiate LVF ictal events may rest on the spacing of specific subicular area targeted for obtaining extracellular signals; in fact in the experiments by Benini and Avoli [23] recording microelectrodes were placed in the subiculum adjacent to the CA1, whereas in the current study, they were positioned more rostrally and closer to the medial EC. If this is the case, it may be suggested that the subiculum receives either a gradient of or distinction between local inputs from the CA1 and the EC [25]. Finally, one cannot exclude the possibility that signals recorded from the subiculum were contaminated by far field effects, namely volume-conducted synchronous neuronal events generated in the EC or other limbic areas comprised in the brain slice [26].

Our results also show that sudden onset ictal events most likely initiate in the EC, whereas those with LVF onset features appear to initiate from close subiculum–EC interactions. However, after cutting the connections between subiculum and EC, both types of ictal events continued to occur in the EC (though with shorter duration than in control) while they either disappeared in the subiculum altogether or manifested as trains of positive going spikes. This discrepancy suggests that the regional specificity is either an oversimplification of the size of the network involved in generating the ictal event, or the spatial resolution of our field recordings was insufficient to catch the 'true' ictal onset region.

Because ictal discharges are modified in both limbic structures, it can be hypothesized that a local EC–subicular circuit plays a role in generating and sustaining ictal activity. Why then, when the circuit is intact, is the EC more likely to initiate sudden onset ictal events whereas

the subiculum is more likely to initiate LVF onset events? This propensity is possibly related to the homeostatic drive exerted by CA1 on the subiculum, controlling hyperexcitablity [27]. This inhibitory drive could increase the likelihood to generate LVF compared to sudden onset events; however, to fully understand the role of EC–subicular interactions in ictogenesis, studies investigating single cell firing dynamics of interneurons and pyramidal cells simultaneously recorded from both regions are required. These studies have the potential to reveal the contribution of different cell types to different onset patterns and identify the region in which cell firing is most correlated to the epileptiform activity identified with field recordings. This approach has been successfully implemented *in vivo* by Toyoda et al. [6,28] in a rat model of temporal lobe epilepsy; it is, however, difficult at this time to extrapolate from these data, which were obtained from a chronic model of epilepsy, to our findings that derive from brain slices acutely treated with convulsant drugs.

4.2. Interictal discharges in subiculum and entorhinal cortex and the role of NMDA receptors

Cutting the connections between EC and subiculum blocked the generation of polyspike discharges in the latter, further suggesting that they are driven by the activity of EC neuronal networks [29]. This effect was accompanied by the appearance in the subiculum of slow interictal events similar to those recorded between LVF onset seizures. Previous studies have shown that these slow interictal events are largely contributed by $GABA_A$ receptor-mediated currents caused by the release of GABA from interneuron terminals [24,29]. This finding is in keeping with the ability of cortical networks to generate synchronous activity reflecting the postsynaptic activation of GABA receptors as reported to occur in human brain slices of the neocortex and subiculum during application of normal medium [11,30,31].

As expected ([24,32]; *cf.*, [33]), blockade of NMDA-receptor mediated signalling prevented ictogenesis in the isolated EC. In addition, during such pharmacological treatment, fast polyspike interictal events were no longer observed and interictal events that were remaining occurred in a less regular pattern. This evidence demonstrates that NMDA receptor signalling plays an important role in ictogenesis as well as in the maintenance of the rhythmicity of fast polyspike interictal activity.

5. Conclusive remarks

Overall, our study demonstrates that the reciprocal circuitry between the EC and subiculum plays an important role in sustaining ictogenesis *in vitro*. When these connections are disrupted, ictal discharges cannot be sustained as efficiently as when EC–subicular connectivity is intact. It is important to emphasize that both sudden- and LVF-onset ictal discharges are equally dependant on reciprocal connections between the subiculum and EC. To better understand the local contribution of the EC–subicular circuit in ictogenesis, further studies should be aimed at analysing the single unit activity generated by specific cell types in both regions.

Acknowledgments

References

1. Perucca P, Dubeau F, Gotman J. Intracranial electroencephalographic seizure-onset patterns: effect of underlying pathology. Brain. 2014; 137:183–96. [PubMed: 24176980]

2. Velasco AL, Wilson CL, Babb TL, Engel J. Functional and anatomic correlates of two frequently observed temporal lobe seizure-onset patterns. Neural Plast. 2000; 7:49–63. [PubMed: 10709214]

3. Bragin A, Azizyan A, Almajano J, Wilson CL, Engel J. Analysis of chronic seizure onsets after intrahippocampal kainic acid injection in freely moving rats. Epilepsia. 2005; 46:1592–8. [PubMed: 16190929]

4. Lévesque M, Salami P, Gotman J, Avoli M. Two seizure-onset types reveal specific patterns of high-frequency oscillations in a model of temporal lobe epilepsy. J Neurosci. 2012; 32:13264–72. [PubMed: 22993442]

5. Avoli M, Panuccio G, Herrington R, D'Anutono M, de Guzman P, Lévesque M. Two different interictal spike patterns anticipate ictal activity in vitro. Neurobiol Dis. 2013; 52:168–76. [PubMed: 23270790]

6. Toyoda I, Bower MR, Leyva F, Buckmaster PS. Early activation of ventral hippocampus and subiculum during spontaneous seizures in a rat model of temporal lobe epilepsy. J Neurosci. 2013; 33:11100–15. [PubMed: 23825415]

7. Bertram EH. Temporal lobe epilepsy: where do the seizures really begin? Epilepsy Behav. 2009; (Suppl 1):32–7.

8. Du F, Whetsell WO Jr, Abou-Khalil B, Blumenkopf B, Lothman EW, Schwarcz R. Preferential neuronal loss in layer III of the entorhinal cortex in patients with temporal lobe epilepsy. Epilepsy Res. 1993; 16(3):223–33. [PubMed: 8119273]

9. Andrioli A, Alonso-Nanclares L, Arellano JI, DeFelipe J. Quantitative analysis of parvalbumin-immunoreactive cells in the human epileptic hippocampus. Neuroscience. 2007; 149:131–43. [PubMed: 17850980]

10. Huberfeld G, Clemenceau S, Cohen I, Pallud J, Wittner L, Navarro V, et al. Epileptiform activities generated in vitro by human temporal lobe tissue. Neurochirurgie. 2008; 54(3):148–58. [PubMed: 18420229]

11. Huberfeld G, Menendez de la Prida L, Pallud J, Cohen I, Le Van Quyen M, Adam C, et al. Glutamatergic pre-ictal discharges emerge at the transition to seizure in human epilepsy. Nat Neurosci. 2011; 14(5):627–34. [PubMed: 21460834]

12. Traub RD, Borck C, Colling SB, Jefferys JG. On the structure of ictal events in vitro. Epilepsia. 1996; 37:879–91. [PubMed: 8814102]

13. Finch DM, Babb TL. Demonstration of caudally directed hippocampal efferents in the rat by intracellular injection of horseradish peroxidase. Brain Res. 1981; 214:405–10. [PubMed: 7237176]

14. Witter MP, Groenewegen HJ. The subiculum: cytoarchitectonically a simple structure, but hodologically complex. Prog Brain Res. 1990; 83(4):47–58. [PubMed: 2392570]

15. Witter MP, Ostendorf RH, Groenewegen HJ. Heterogeneity in the dorsal subiculum of the rat. Distinct neuronal zones project to different cortical and subcortical targets. Eur J Neurosci. 1990; 2:718–25. [PubMed: 12106290]

16. Canteras NS, Swanson LW. Projections of the ventral subiculum to the amygdala, septum, and hypothalamus: a PHAL anterograde tract-tracing study in the rat. J Comp Neurol. 1992; 324:180–94. [PubMed: 1430328]

17. Witter MP, Groenewegen HJ, Lopes da Silva FH, Lohman AH. Functional organization of the extrinsic and intrinsic circuitry of the parahippocampal region. Prog Neurobiol. 1989; 33:161–253. [PubMed: 2682783]

18. Hjorth-Simonsen A. Projection of the lateral part of the entorhinal area to the hippocampus and fascia dentata. J Comp Neurol. 1972; 146:219–32. [PubMed: 5073889]

19. Witter MP, Groenewegen HJ. Laminar origin and septotemporal distribution of entorhinal and perirhinal projections to the hippocampus in the cat. J Comp Neurol. 1984; 22:372–85.

20. Van Groen T, Lopes da Silva FH. Organization of the reciprocal connections between the subiculum and entorhinal cortex in the cat: an electrophysiological study. J Comp Neurol. 1986; 251(1):111–20. [PubMed: 3760255]

21. Shao LR, Dudek FE. Repetitive perforant-path stimulation induces epileptiform bursts in minislices of dentate gyrus from rats with kainate-induced epilepsy. J Neurophysiol. 2011; 105(2): 522–7. [PubMed: 21148094]

22. Steward O, Scoville SA. Cells of origin of entorhinal cortical afferents to the hippocampus and fascia dentate of the rat. J Comp Neurol. 1976; 169(3):347–70. [PubMed: 972204]

23. Benini R, Avoli M. Rat subicular networks gate hippocampal output activity in an in vitro model of limbic seizures. J Physiol. 2005; 566(3):885–900. [PubMed: 15932889]

24. Avoli M, Barbarosie M, Lucke A, Nagao T, Lopantsev V, Köhling R. Synchronous GABA-mediated potentials and epileptiform discharges in the rat limbic system in vitro. J Neurosci. 1996; 16:3912–24. [PubMed: 8656285]

25. Naber PA, Lopes da Silva FH, Witter MP. Reciprocal connections between the entorhinal cortex and the subiculum are in register with the projections from CA1 to the subiculum. Hippocampus. 2001; 11(2):99–104. [PubMed: 11345131]

26. Inaba Y, Avoli M. Volume-conducted epileptiform events between adjacent neocortical slices in an interface tissue chamber. J Neurosci Methods. 2006; 151:287–90. [PubMed: 16143402]

27. Sah N, Sikdar SK. Transition in subicular burst firing neurons from epileptiform activity to suppressed state by feed forward inhibition. Eur J Neurosci. 2013; 38(4):2542–56. [PubMed: 23725217]

28. Toyoda I, Fujita S, Thamattoor AK, Buckmaster PS. Unit activity of hippocampal interneuron's before spontaneous seizures in an animal model of temporal lobe epilepsy. J Neurosci. 2015; 35(16):6600–18. [PubMed: 25904809]

29. Lopantsev V, Avoli M. Laminar organization of epileptiform discharges in the rat entorhinal cortex in vitro. J Physiol. 1998; 509:785–96. [PubMed: 9596800]

30. Köhling R, Höhling JM, Straub H, Kuhlmann D, Kuhnt U, Tuxhorn I, et al. Optical monitoring of neuronal activity during spontaneous sharp waves in chronically epileptic human neocortical tissue. J Neurophysiol. 2000; 84(4):2161–5. [PubMed: 11024103]

31. Cohen I, Navaro V, Clemenceau S, Baulac M, Miles R. On the origin of interictal activity in human temporal lobe in vitro. Science. 2002; 298:1418–21. [PubMed: 12434059]

32. Lopantsev V, Avoli M. Participation of $GABA_A$-mediated inhibition in ictal-like discharges in the rat entorhinal cortex. J Neurophysiol. 1998; 79:352–60. [PubMed: 9425204]

33. Avoli M, de Curtis M. GABAergic synchronization in the limbic system and its role in the generation of epileptiform activity. Prog Neurobiol. 2011; 95(2):104–32. [PubMed: 21802488]
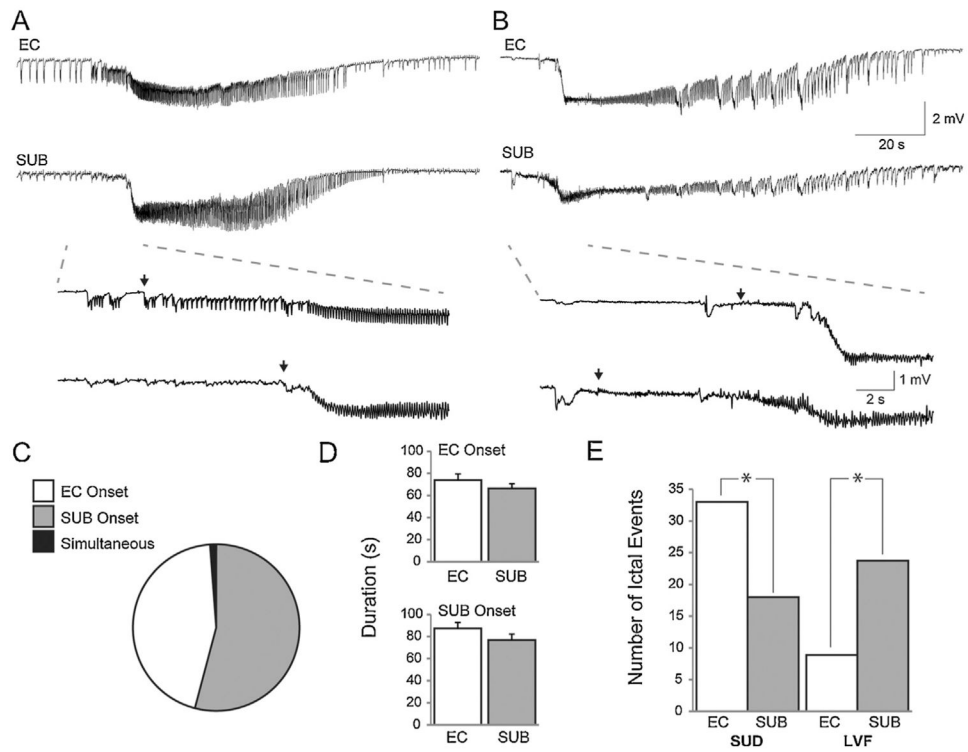
Fig. 1.
Different ictal onset patterns recorded from the EC and subiculum. (A) Example of a sudden onset ictal event with the onset period expanded below. Single arrows represent ictal onset points. (B) Example of an LVF onset ictal event, again with the onset period expanded below. (C) Pie chart representing the proportion of ictal events initiating in subiculum, EC, or simultaneously in both regions. (D) Bar graphs showing the duration of ictal events in the EC and subiculum based on the region in which they were first detected. (E) Proportion of sudden onset and LVF onset ictal events that appeared to initiate in either the EC (white) or subiculum (grey) (*$P < 0.001$, Fisher's Exact Test).
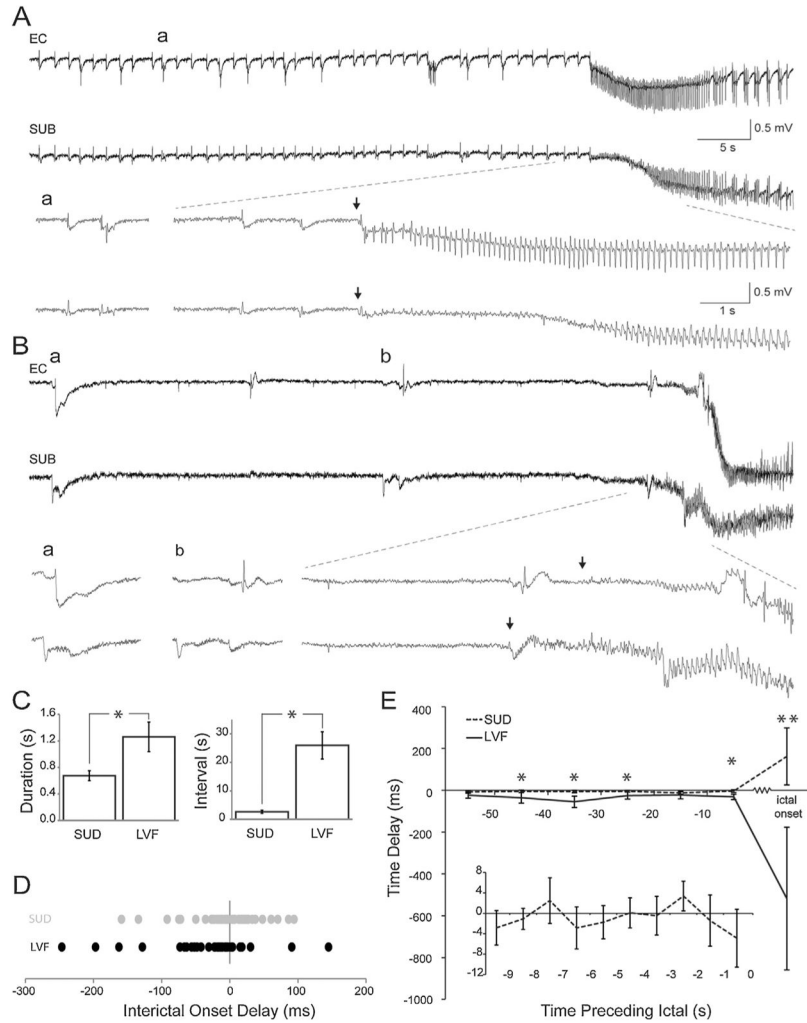
Fig. 2.
Delays between interictal discharges in relation to the time preceding sudden and LVF ictal onset patterns. (A) Frequent polyspike interictal discharges precede a sudden onset ictal event. Single arrows represent ictal onset points. (B) Interictal discharges preceding an LVF onset ictal event. (C) Bar graphs showing the duration and the interval of occurrence of interictal events based on the ictal onset pattern they are associated with. (D) Chart showing the distribution of time delays between the entorhinal cortex and subiculum at the interictal event immediately preceding the ictal event. Negative values indicate that the subiculum leads the entorhinal cortex whereas positive values indicate that the entorhinal cortex leads the subiculum. Each dot represents a single interictal event. (E) Line graph depicting average delays between synchronized interictal events in 10 s time bins preceding the ictal event. Time 0 represents the interictal event immediately preceding the ictal event. Positive values indicate that the event initiates in the entorhinal cortex and negative values indicate that the event initiates in the subiculum. The inset shows an expansion of the time bin preceding ictal onset for sudden onset events only (*$P < 0.05$; **$P < 0.001$).
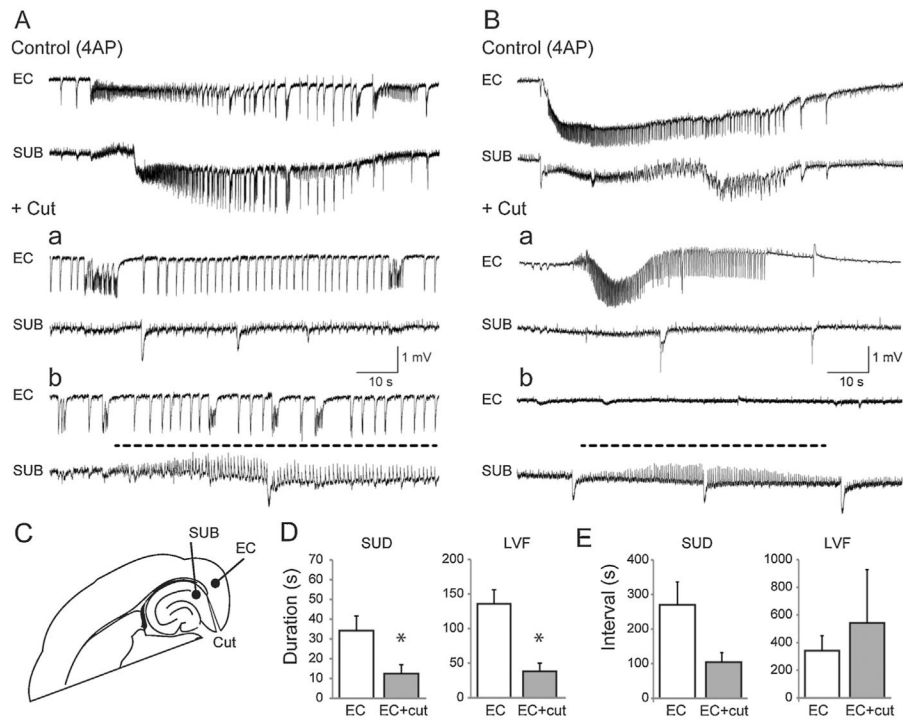
Fig. 3.
Ictal synchronization between structures. Synchronicity between the entorhinal cortex and subiculum can be manipulated by severing connections between the regions. (A) Traces of a sudden onset ictal event during control (4AP only) conditions and after cutting the connections between the subiculum and entorhinal cortex. (B) Traces depicting the change in synchronization between the entorhinal cortex and subiculum in a slice characterized by LVF ictal events. In both panels A and B, the dotted line highlights the trains of positive-going spikes that occur in the subiculum after the cut. (C) Schematic showing the location of the "cut" and the electrode placement. (D) Bar graphs indicating the change in duration of ictal events following the cut in slices characterized by either sudden or LVF onset patterns. (E) Bar graphs showing the change in interval between either sudden onset or LVF ictal events following the cut (*$P < 0.05$).
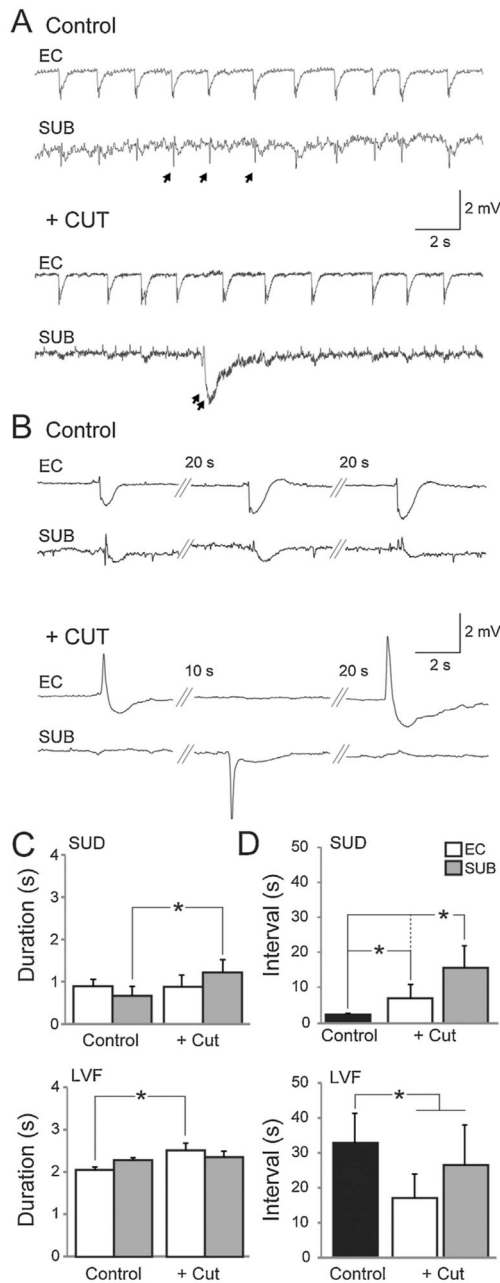
Fig. 4.
Interictal synchronization between structures. Synchronicity between interictal events recorded in the subiculum and entorhinal cortex can be modulated by severing connections. (A) Representative traces of interictal events recorded during control (4AP) conditions and after cutting the connections between the subiculum and entorhinal cortex in a slice characterized by sudden onset ictal events. Single arrows point to fast polyspike interictal discharges and double arrows point to long lasting interictal discharges. (B) Interictal events recorded from a slice characterized by LVF ictal events. (C, D) Bar graphs showing the

change in duration and interval, respectively, of interictal events recorded from slices characterized by LVF or sudden onset ictal events (*$P < 0.001$).
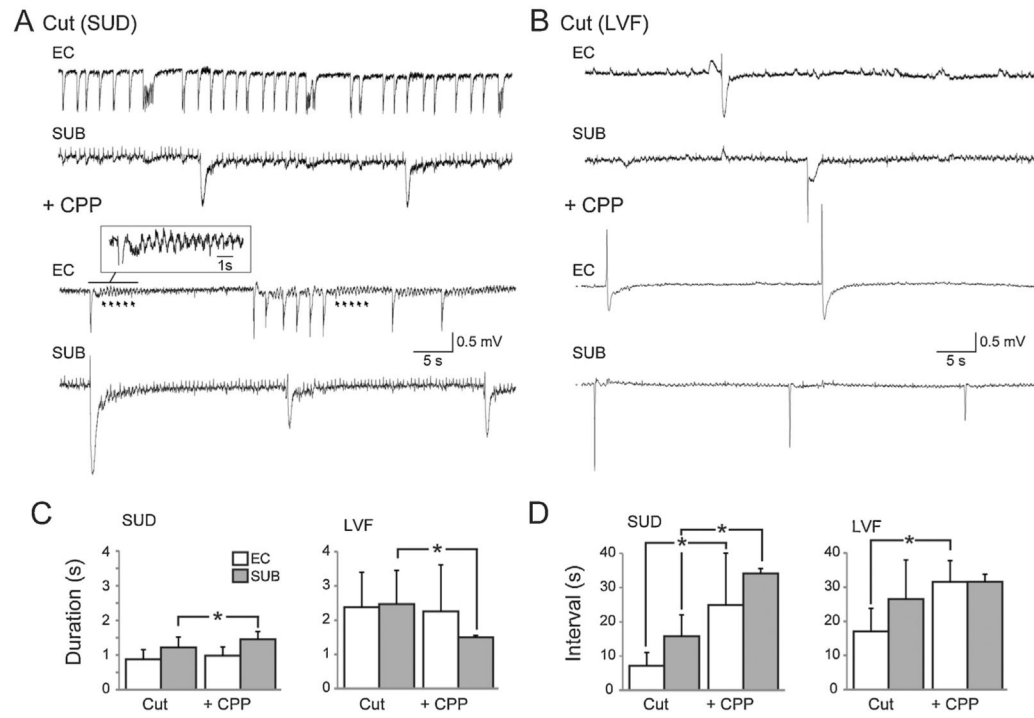
Fig. 5.
Blockade of NMDA-receptor mediated signalling. Glutamatergic activity plays an important role in epileptiform synchronization. (A, B) Representative traces showing the effects of CPP on slices where connections between EC and subiculum are severed. In panel A, the expanded inset shows activity that occurs at approximately 2 Hz which can be revealed with the application of CPP. (C, D) Bar graphs showing the changes in duration and interval in slices before (4AP + Cut) and after the application of CPP (*$P < 0.05$).